

A Ratiometric Near-Infrared Fluorescent Probe for Quantification and Evaluation of Selenocysteine-Protective Effects in Acute Inflammation

Xiaoyue Han, Xinyu Song, Fabiao Yu,* and Lingxin Chen*

Selenocysteine (Sec) is a primary kind of reactive selenium species in cells whose antioxidant roles in a series of liver diseases have been featured. However, it is difficult to determine Sec in living cells and in vivo due to its high reactivity and instability. This work reports a ratiometric near-infrared fluorescent probe (Cy-SS) for qualitative and quantitative determination of Sec in living cells and in vivo. The probe is composed of heptamethine cyanine fluorophore, the response unit bis(2-hydroxyethyl) disulfide, and the liver-targeting moiety D-galactose. Based on a detection mechanism of selenium–sulfur exchange reaction, the concentrations of Sec in HepG2, HL-7702 cells, and primary mouse hepatocytes is determined as $3.08 \pm 0.11 \times 10^{-6}$ M, $4.03 \pm 0.16 \times 10^{-6}$ M and $4.34 \pm 0.30 \times 10^{-6}$ M, respectively. The probe can selectively accumulate in liver. The ratio fluorescence signal of the probe can be employed to quantitatively analyze the fluctuation of Sec concentrations in cells and mice models of acute hepatitis. The experimental results demonstrate that Sec plays important antioxidant and anti-inflammatory roles during inflammatory process. And the levels of intracellular Sec have a close relationship with the degree of liver inflammation. The above imaging detections make this new probe a potential candidate for the accurate diagnosis of inflammation.

1. Introduction

Cellular antioxidant systems prevent cells from oxidative damage. The intracellular antioxidant mechanisms involve small-molecule antioxidants, such as reactive sulfur and selenium groups. The biological protective effects of reactive sulfur and selenium species are commonly attributed to scavenging and enzymatic decomposition of excessive reactive oxygen species (ROS).^[1] However, the antioxidant behaviors deriving from reactive sulfur and selenium antioxidants are quite different. The antioxidative mechanism of selenium antioxidant is featured to direct scavenge ROS via a ping-pang mechanism.^[2] In vivo reactive selenium

species (RSeS) are mainly presented as organic selenium-containing amino acids, such as selenocysteine (CysSeH, Sec), selenogluthathione (GSeH), cysteine selenopersulfide (CysSSeH), glutathione selenopersulfide (GSSeH), Se-methylselenocysteine, selenomethionine, and so on.^[3] They are usually incorporated into proteins as the active sites of enzymes, such as glutathione peroxidases (GPx) and thioredoxin reductases (Trx).^[4] There are at least 25 different selenoproteins (SePs) in humans. These SePs have extensive physiological functions ranging from reducing oxidative stress, endoplasmic reticulum stress, and inflammation to protecting the endothelium and regulating vascular tone.^[5] The lack of selenium results in poor immune function and high cancer risk. But the higher selenium supplementation leads to increasing risk of type 2 diabetes and acute or chronic selenium toxicity,^[6] because high concentration of RSeS can conversely enhance intracellular O_2^- levels

via transferring an electron to O_2 .^[7] Therefore, the right supply and demand of RSeS are essential for health.

Inflammation is a biological phenomenon which provides host defense against infection or invasion. Once inflamed, the activated immune cells induce oxidative burst which results in high levels of ROS within minutes. If the homeostasis between inflammatory and anti-inflammatory is disrupted, the uncontrollable inflammation has been considered to be a potential incentive in the early stages of cancer. During these redox-based cellular processes, RSeS are involved as modulators of inflammatory response.^[8] Among all these RSeS, Sec has been considered to be the first-line against oxidative stress in cellular antioxidant defense system. It performs the powerful nucleophilicity ability, readily antioxidation capability, favorable kinetic properties of the selenium center, as well as its potential property to chelate redox-active metal ions.^[7] Sec also assumes the responsibility for synthesis of selenium-dependent antioxidants and repair of proteins.^[8] Adequate levels of Sec can regulate excessive immune responses and uncontrollable inflammation. The deficiency of Sec will lead to negatively impact on immune cells during activation, differentiation, and proliferation.^[9] Given the unique property and high reactivity of Sec in the regulation of inflammatory processes, selenium-containing drugs have been manufactured to be metabolized as Sec for the

Dr. X. Han, Dr. X. Song, Prof. F. Yu, Prof. L. Chen
Key Laboratory of Coastal Environmental Processes and
Ecological Remediation
Yantai Institute of Coastal Zone Research
Chinese Academy of Sciences
Yantai 264003, China
E-mail: fbyu@yic.ac.cn; lxchen@yic.ac.cn

Dr. X. Han
University of Chinese Academy of Sciences
Beijing 100049, China

DOI: 10.1002/adfm.201700769

treatment of inflammation in liver.^[10] For instance, the drug 3-alkynyl selenophene exhibits protective and anti-inflammatory effects on acute liver injury which is induced by D-galactosamine and lipopolysaccharide.^[11] Diphenyl diselenide can protect rats from acute liver damage which is caused by 2-nitropropane.^[12] As a more immediate drug supplement, selenocystine can prevent carbon tetrachloride (CCl₄) induced acute hepatic injury in rats.^[13] Due to the special physiological function of the liver, the concentration of Sec must be maintained at high level.^[3,4] Therefore, it is necessary to evaluate the level of Sec which has a close relationship between the redox statuses and inflammatory state of the liver.

Fluorescent probes have proven their potential applications in the field of bioimaging analysis owing to their highly sensitivity, excellent selectivity, less invasiveness, rapid response, as well as high spatial and temporal resolution.^[14] Many efforts have been made to develop fluorescent probes for the detection of biothiols in living cells, but a few achievements have been reported for imaging physiological relevant Sec.^[15] The most preferred detection method for Sec is the mechanism of nucleophilic aromatic substitution.^[16] The nucleophilic reaction with aromatic diamine is another detection method.^[17] Although these probes are elegantly established for the detection of Sec, most of them are vaguely described their selectivity for free bioselenols (represented as Sec) against SePs.^[15–17] Sec is the precursor of SePs. The physiological functions of Sec and SePs are discriminate. Moreover, the distributions of RSeS (represented as Sec) and SePs are rich in liver. Until now, there is no fluorescent probe which provides organ-targeting ability for the detection of Sec in liver. The design of the probe which can qualitatively and quantitatively determine the accurate concentration of Sec is more challengeable. Therefore, we strive to develop a sensitive and rapid probe for the direct identification and measurement of Sec in liver excluding SePs.

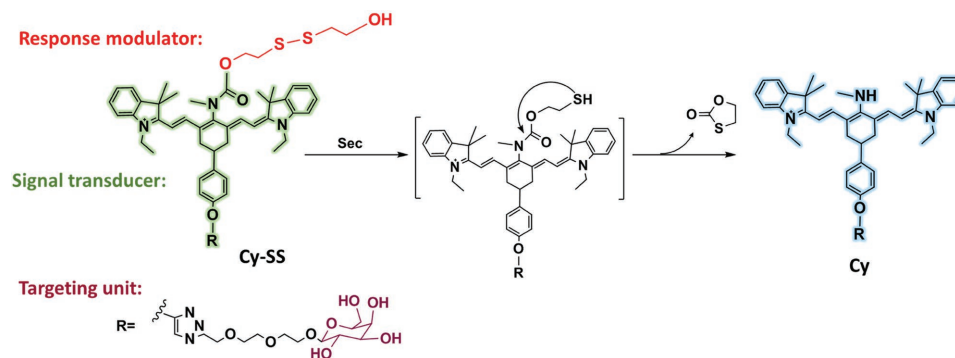
Herein, we conceived a liver-targeting ratiometric near-infrared (NIR) fluorescent probe (Cy-SS) for the selective detection of Sec in living cells and in vivo (**Scheme 1**). Our strategy was based on a selenium–sulfur exchange reaction, which was employed in our previous findings on the quantitation of intramolecular cysteine hydropersulfide (Cys-SSH).^[18] We chose heptamethine cyanine as NIR fluorophore, bis(2-hydroxyethyl) disulfide as Sec response modulator, and D-galactose as liver-targeting unit. The fluorescent response of Cy-SS toward Sec could rapidly complete within minutes in the present of millimolar concentration of

intracellular glutathione (GSH). This rapid response characteristic played a crucial role in the fast detection on account of avoiding interference from other biothiols in biological systems. The test results enabled the probe to qualitatively and quantitatively detect the whole Sec levels in HL-7702 cells (human normal liver cell line), HepG2 cells (human hepatocellular liver carcinoma cell line), and primary mouse hepatocytes. Utilizing the cell and mice models of acute hepatitis, we evaluated the therapeutic effects of organoselenium drug selenocystine. Moreover, taking advantage of Cy-SS, we found the fluctuations of Sec levels in cells and in vivo when against inflammation.

2. Result and Discussion

2.1. Molecular Design of Cy-SS for Sec

The first issue to overcome is how to eliminate the interferences from reactive sulfur species (RSS) which behave the similar characteristics of nucleophilic reaction with RSeS. Additionally, the whole millimolar concentrations of RSS in cells make the detection even more challenging.^[19] However, there are quite distinct pK_a between biothiols (RSH) and bioselenols (RSeH). The pK_a of RSeH is ≈5.2, which makes them stronger acidic compared to cysteine (Cys, pK_a = 8.29) and GSH (pK_a = 8.75) at physiological pH (7.40).^[20] In cells, almost all RSeH exist as the deprotonated anion (RSe[−]), while RSH exist as their protonated forms. Therefore, RSeH perform full nucleophilic capacity compared to RSH. In our previous studies, we employed selenium–sulfur exchange reaction^[21] to visualize and quantify the levels of persulfides in cells and in vivo.^[18] It is promising that the disulfide can also be more rapidly reduced by the stronger nucleophilic RSeH than RSH.^[21] In this work, we strive to develop a new ratiometric near-infrared fluorescent probe for accurate qualitative and quantitative analysis of Sec in living cells and in vivo. The overall design strategy is shown in Scheme 1. We introduced a reactive disulfide (2,2′-dithiodiethanol) as the Sec response moiety. Although the similar disulfide can be used for the detection of biothiols in cells,^[22] our experimental results offered a very slow response rate toward biothiols. Only a negligible amount had been cleaved after 12 h incubation with biothiols (Figure S2, Supporting Information). Cys-SSH whose pK_a was ≈4.34 could not cause the interference. The slow reaction rates for exchange reactions are attributed



Scheme 1. Schematic representation of the reaction of Cy-SS with Sec.

to the kinetic and thermodynamic properties of biothiols with their disulfide-containing compounds.^[21,23] For the selective detection of Sec in cells, the interferences from SePs, such as GPx and Trx, must be eliminated.^[24] We hypothesized that the introduction of response moiety at meso-chloro site of NIR heptamethine cyanine fluorophore would result in a bulky steric hindrance, which blocked the reaction between Cy-SS and SePs. Moreover, the facile modulation of different electron-donating donors on cyanine fluorophore could lead to internal charge transfer (ICT)-induced blue or red shifts in the emission spectrum.^[25] As shown in Scheme 1, the reduction of disulfide bond by Sec triggered a fast intramolecular cyclization. After the cleavage of neighboring amide bond, the released fluorophore exhibited a larger spectral blue shift. As known, the ratiometric fluorescence probes which take advantage of the ratio of the spectra at two or more emission bands can eliminate disturbance caused by the excitation and emission efficiency, as well as variable factors derived from uneven loading or inhomogeneous distribution of the probes and environmental conditions. The NIR fluorescence can maximize tissue penetration, minimizing the absorbance of heme in hemoglobin and myoglobin, water, and lipids, simultaneously. Liver is a predominant innate immunologic and essential metabolic organ in vivo. Liver damage ranges from acute hepatitis to hepatocellular carcinoma whose progression is close related to oxidative stress.^[26] In order to evaluate the protective effects of Sec in liver, we introduced a galactose-terminated ligand into our fluorescence platform, because asialoglycoprotein receptor (ASGP-R)

specifically expresses on the plasma membrane of mammalian hepatocytes and selectively accepts the terminal galactose residues on desialylated glycoproteins.^[22] Now, the desirable probe Cy-SS was completely constructed. The synthesis routes of probe are described in Supporting Information in detail.

2.2. Spectral Properties of Probe Cy-SS

The spectral properties of Cy-SS (10×10^{-6} M) were examined in 4-(2-hydroxyethyl)-1-piperazineethanesulfonic acid (HEPES) solution (10×10^{-3} M, pH 7.4) with different Sec concentrations (0 – 20×10^{-6} M). The probe displayed sensitive absorption and fluorescence responses toward Sec. Upon reaction with Sec, the maximum absorption wavelength at 782 nm ($\epsilon_{782 \text{ nm}} = 5.60 \times 10^4 \text{ M}^{-1} \text{ cm}^{-1}$) decreased, while a new absorption peak at 610 nm ($\epsilon_{610 \text{ nm}} = 3.26 \times 10^4 \text{ M}^{-1} \text{ cm}^{-1}$) emerged (Figure 1a). Correspondingly, the maximum fluorescence wavelength shifted from 800 nm ($\Phi = 0.06$) to 750 nm ($\Phi = 0.11$) (Figure 1b,c). The ratiometric fluorescence values ($F_{750 \text{ nm}}/F_{800 \text{ nm}}$) gradually increased and varied from 0.16 to 20.97 as the concentrations of Sec changed from 0 to 20×10^{-6} M (Figure 1d). There was a good linearity between logarithm of the ratio ($F_{750 \text{ nm}}/F_{800 \text{ nm}}$) and the Sec concentrations (Figure 1d). The linear regression equation was $\lg(F_{750 \text{ nm}}/F_{800 \text{ nm}}) = 0.08975 \times [\text{Sec}] (\times 10^{-6} \text{ M}) - 0.7085$, $r = 0.9912$. The experimental detection limit was estimated to be 0.09×10^{-6} M. These results indicated that Sec could be qualitatively and quantitatively detected using the probe Cy-SS.

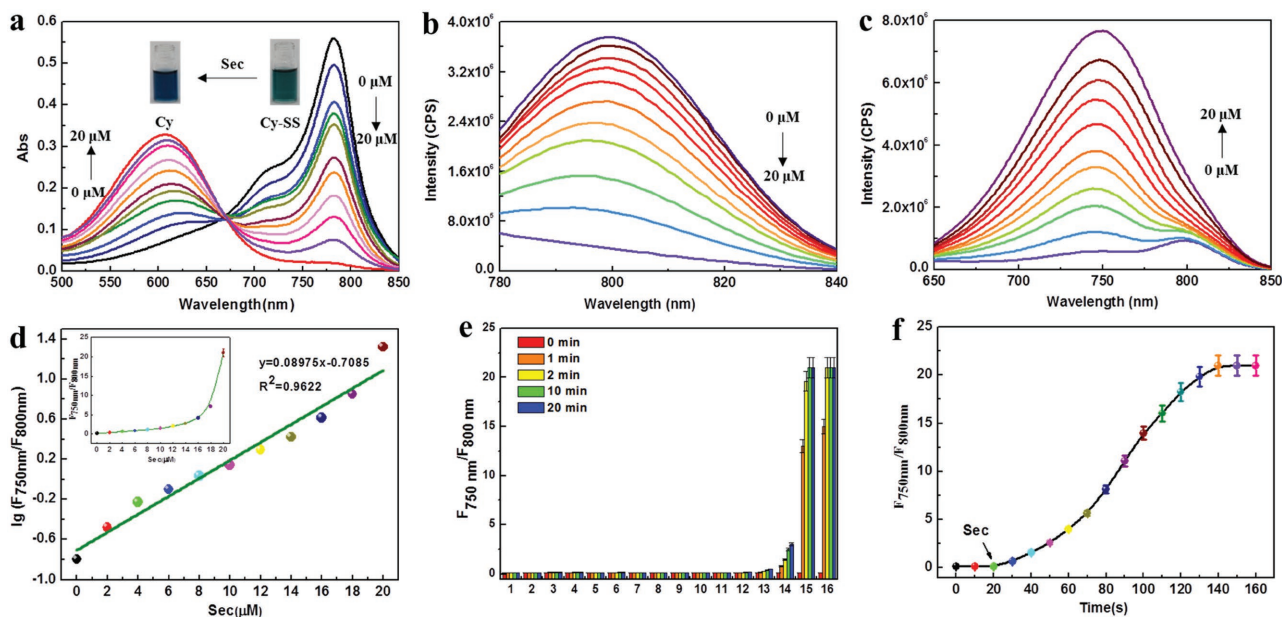


Figure 1. Spectral properties and selectivity of Cy-SS. a) Dose-dependent absorbance spectra of Cy-SS (10×10^{-6} M) toward Sec. Data were recorded after 2 min incubated with increasing concentration of Sec (0 – 20×10^{-6} M) at 37°C in HEPES (pH 7.4, 10×10^{-3} M). b) $\lambda_{\text{ex}} = 720$ nm. c) $\lambda_{\text{ex}} = 610$ nm. Dose-dependent emission spectra of Cy-SS (10×10^{-6} M) toward Sec. All the above experimental conditions are the same as those in (a). d) The linear relationship between the $\lg(F_{750 \text{ nm}}/F_{800 \text{ nm}})$ and Sec. Insert: Intensity ratio of Cy-SS change as a function of Sec. e) Time-dependent fluorescent ratio ($F_{750 \text{ nm}}/F_{800 \text{ nm}}$) response of Cy-SS to various reactive species. 1, blank; 2, 20×10^{-6} M NaHS; 3, 200×10^{-6} M Cys; 4, 10×10^{-3} M GSH; 5, 20×10^{-6} M Hcy; 6, 20×10^{-6} M Cys-SSH; 7, 20×10^{-6} M NAC; 8, 20×10^{-6} M ascorbic acid; 9, 20×10^{-6} M Se-methylselenocysteine; 10, 20×10^{-6} M selenocysteine; 11, 20×10^{-6} M selenomethionine; 12, 20×10^{-6} M GPx; 13, 20×10^{-6} M TrxR; 14, 20×10^{-6} M Na_2SeO_3 ; 15, 20×10^{-6} M GSeH; 16, 20×10^{-6} M Sec. f) Time dependent fluorescent ratio of probe Cy-SS toward Sec during 0–160 s. Sec was added at the reaction time of 20 s. $F_{750 \text{ nm}}$: $\lambda_{\text{ex}} = 610$ nm, $\lambda_{\text{em}} = 750$ nm; $F_{800 \text{ nm}}$: $\lambda_{\text{ex}} = 720$ nm, $\lambda_{\text{em}} = 800$ nm. The experiments were repeated three times and the data were shown as mean (\pm S.D.).

2.3. Selectivity and Effects on pH

High selectivity and stable properties at physiological pH range are required features for a newly designed fluorescent probe. The selectivity tests for RSeS showed that Sec and GSeH rapidly underwent the sulfur–selenium exchange reaction and triggered the ICT mechanism. Because Sec was the primary species in RSeS, we singled out Sec as a representative for further examination in this work. Considering the rapid metabolism and unstable properties of Sec, the reaction kinetic of Cy-SS toward Sec was performed. The time course of Sec inducing sulfur–selenium reaction was investigated under physiological condition. As shown in Figure 1f, the ratio-fluorescence signal response to Sec would reach saturation within 120 s, indicating our probe could be used as a unique real-time bioimaging tool for the detection of intracellular Sec. Se-methylselenocysteine, selenocystine, selenomethionine, and sodium selenite (Na_2SeO_3) gave no interference. By the way, CysSSeH and GSSeH are presented in Seps as the active sites.^[27] Due to steric hindrance, our probe could not respond to Seps (such as GPx and Trx). Other reactive biological species, such as sodium hydrosulfide (NaHS), Cys, GSH, homocysteine (Hcy), *N*-acetyl-L-cysteine (NAC), Cys-SSH, ascorbic acid, reactive oxygen species, reactive nitrogen species, anions, and metal ions could not introduce interference under the given testing conditions (Figure 1e, Figure S3a,b, Supporting Information). These results demonstrated that our probe Cy-SS could meet the requirements for the selective detection of Sec. The effects of pH on Cy-SS were studied in the absence and presence of Sec (Figure S3, Supporting Information). These results indicated that the probe could be employed for the detection of Sec under physiological pH (pH = 7.4).

2.4. Quantification of Sec in Living Cells

To evaluate the potential utility of Cy-SS for qualitative and quantitative analysis intracellular Sec, HL-7702 cells, HepG2 cells, and primary mouse hepatocytes (female BALB/c mice) were selected as test models. All experimental procedures were conducted in conformity with institutional guidelines for the care and use of laboratory animals, and protocols were approved by the Institutional Animal Care and Use Committee in Binzhou Medical University, Yantai, China. Before cell imaging applications, the cytotoxicity of the probe was evaluated via 3-(4,5-dimethyl-2-thiazolyl)-2,5-diphenyl-2-H-tetrazolium bromide (MTT) assays. Experimental results demonstrated low cytotoxicity to the three kinds of cells (Figure S5, Supporting Information). The cell imaging experiments were performed utilizing laser scanning confocal microscope. Cells were incubated with 10×10^{-6} M Cy-SS at 37 °C for 5 min before imaging. The ratio fluorescence images were reconstructed from two channels, channel 1: $\lambda_{\text{ex}} = 730$ nm, $\lambda_{\text{em}} = 750\text{--}800$ nm; channel 2: $\lambda_{\text{ex}} = 635$ nm, $\lambda_{\text{em}} = 690\text{--}740$ nm. Pseudocolor ratio images were used to indicate the ratio of emission intensity of channel 2 versus channel 1. As shown in Figure 2a,b, the ratio fluorescence intensities increased during 0–90 s in HepG2, HL-7702 cells and primary hepatocytes. However, the three types of cells offered distinguishable signals which were

related with their distinct Sec generation abilities. We selected the time point at 90 s to access the Sec concentrations in the three kinds of cells. $F_{\text{channel 1/channel 2}} = 0.37, 0.45$ and 0.48 for HepG2, HL-7702 and primary hepatocytes, respectively. Based on the equation in Figure 1d, the Sec concentrations were calculated as $3.08 \pm 0.11 \times 10^{-6}$ M, $4.03 \pm 0.16 \times 10^{-6}$ M, and $4.34 \pm 0.30 \times 10^{-6}$ M correspondingly. Flow cytometry has been widely used in cellular quantitative analysis owing to its high precision with large amount of analyzed samples. The flow cytometry analysis was carried out at time points of 0 and 90 s (Figure 2d). The concentrations of Sec in HepG2, HL-7702 cells and primary hepatocytes were determined as $3.09 \pm 0.12 \times 10^{-6}$ M, $4.04 \pm 0.18 \times 10^{-6}$ M, $4.36 \pm 0.20 \times 10^{-6}$ M, respectively (Figure 2e). To verify the potency and accuracy quantitative analysis of the probe, LC–MS/MS analysis was further performed to quantify Sec labeled by iodoacetamide.^[28] The LC–MS/MS analysis results were $3.11 \pm 0.15 \times 10^{-6}$ M in HepG2 cells, $4.08 \pm 0.26 \times 10^{-6}$ M in HL-7702 cells, $4.48 \pm 0.34 \times 10^{-6}$ M in primary hepatocytes, respectively (Figure S7 and Table S1, Supporting Information). The results obtained from ratio images, flow cytometry, and LC–MS/MS were well consistent, which confirmed the further quantitative application of our probe Cy-SS in living cells and in vivo.

2.5. Sec Detection in Cell Models of Acute and Chronic Hepatitis

Encouraged by the successful application for Sec quantification in living cells, the probe Cy-SS was further employed to detect the fluctuations of Sec concentrations in cells. Sec behaves both as an antioxidant and anti-inflammatory agent in liver. Its concentration can be expected to be influenced by inflammation.^[29] As signal proteins to mediate the inflammation response, pro-inflammatory cytokines are divided into two types: those involved in acute inflammation and those responsible for chronic inflammation.^[30] The cell models of acute and chronic inflammation were induced by pro-inflammatory cytokines: IL-1 β and INF- γ , respectively. Cells were incubated with 10×10^{-6} M Cy-SS at 37 °C for 5 min before imaging. All the cell imaging results in Figure 3a,b were obtained at the time point of 90 s. The cells in group a exhibited high ratio fluorescence signal indicating the high levels of Sec in living HL-7702 cells. The cells in group b were pretreated with 60 ng mL⁻¹ IL-1 β for 24 h to induce acute inflammation,^[31] which could inhibit the expression of SePs and promote the depletion of Sec.^[32] Selenocystine has been recommended as a direct supplement of Sec for the prevention and treatment of oxidative stress related diseases, such as inflammation.^[33] The cells of group c in Figure 3a were incubated with 50×10^{-6} M selenocystine for 2 h before stimulated by IL-1 β . The higher ratio fluorescence of group c than group b indicated higher Sec concentration in cells, which was benefited from the protective roles of Sec. The HL-7702 cells in group d were incubated with 60 ng mL⁻¹ pro-inflammatory cytokines INF- γ for 24 h to induce chronic inflammatory response. Then the ratio fluorescence of group b and d were compared. Group d provided a stronger ratio signal than that of group b. Next, the cells in group e were firstly added 50×10^{-6} M selenocystine for 2 h, then stimulated by INF- γ to induce chronic inflammatory

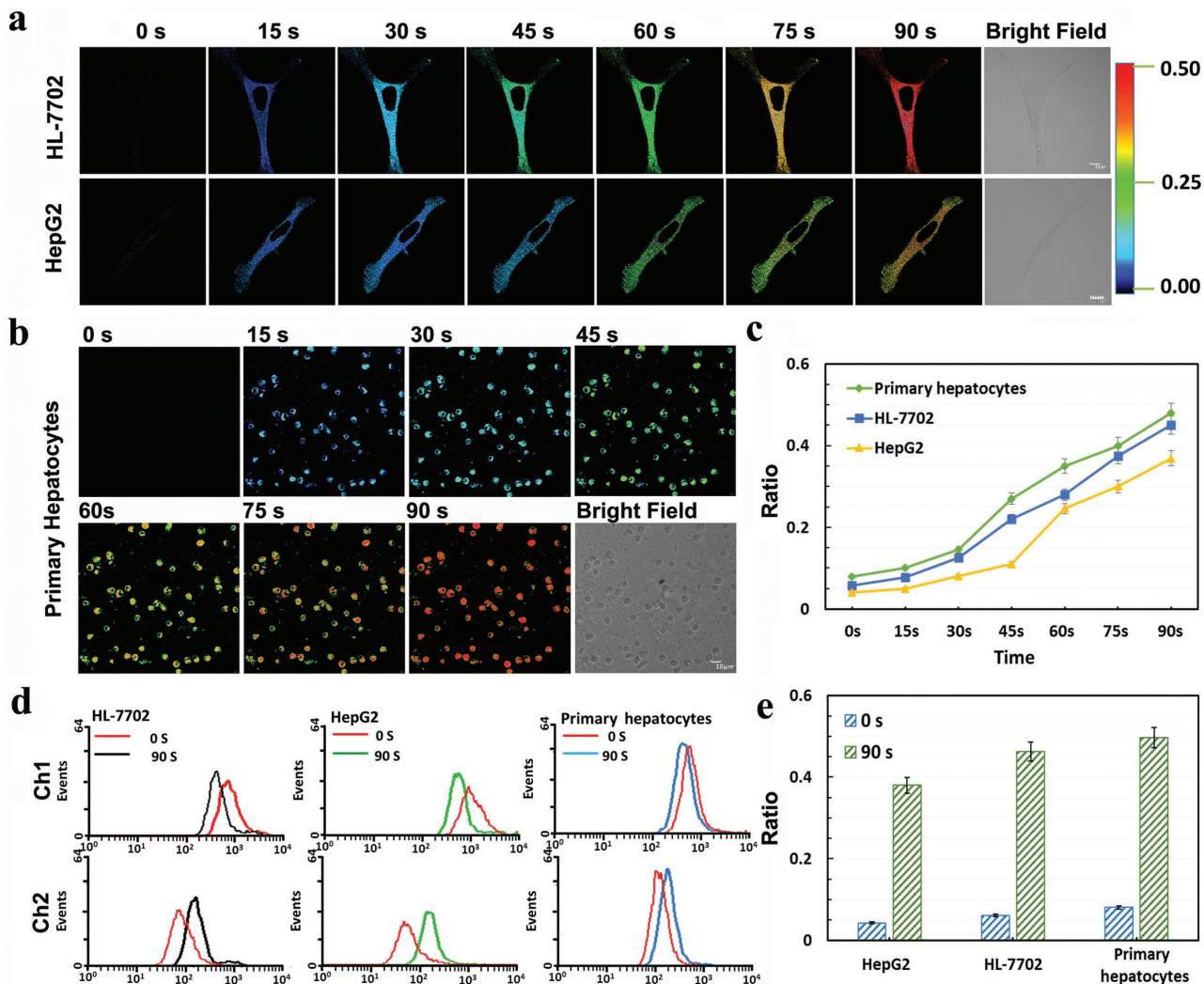


Figure 2. Quantitative application of Cy-SS to endogenous Sec generation in living HepG2, HL-7702 cells and primary hepatocytes by confocal imaging and flow cytometry analysis. Pseudocolor ratio images of endogenous Sec generation in a) HL-7702 and HepG2 cells, and b) primary hepatocytes at different time points: 0, 15, 30, 45, 60, 75, and 90 s by confocal laser-scanning microscope with an objective lens ($\times 60$). Fluorescence collection windows for channel 1: 750–800 nm ($\lambda_{\text{ex}} = 730$ nm), channel 2: 690–740 nm ($\lambda_{\text{ex}} = 635$ nm). c) Plots of average ratio intensities of Cy-SS against time. d) Flow cytometry analysis and e) corresponding mean ratio intensity at time points: 0 and 90 s. The experiments were repeated three times and the data were shown as mean (\pm S.D.).

response before imaging. There obtained a strong ratio fluorescence signal for group e. According to these results, the treatment of $\text{INF-}\gamma$ and $\text{IL-1}\beta$ for HL-7702 cells could lead to different degrees of inflammation which resulted in different levels of oxidative stress damage. As a result of this, the apoptosis and necrosis percentages were ordered as: group $b > d > c > e > a$ (Figure 3e). Following the ratio imaging results of group a, b, c, d, and e, the levels of Sec were arranged from high to low as group $a > e > c > d > b$ (Figure 3b). All the results evidently illustrated that Sec played protective and regulatory roles in inflammation. The changes of ratio fluorescent signals in group a–e were further verified by flow cytometry analysis. As shown in Figure 3c,d, we obtained the same order of Sec levels as having been provided in Figure 3a,b. The above experiments demonstrated that our probe Cy-SS could be used to evaluate Sec levels in the cell models of acute and chronic inflammation.

The nuclear factor kappa-B (NF- κ B) is a transcriptional factor which is of pivotal importance in immune and pro-inflammatory response. This signaling pathway has been associated with enhanced inflammatory response and its activation has been significantly correlated with pro-inflammatory cytokines.^[34] To check the relationship between the concentration of intracellular Sec and inflammation, we next assessed the expression of NF- κ B subunit p65 protein in group a–e exploiting immunofluorescence analysis method. The rabbit antiphospho-NF κ B p65(Ser276)/fluorescein isothiocyanate (FITC) was introduced to selectively response to the NF- κ B subunit p65 protein. As illustrated in Figure 3f, the sequence of NF- κ B subunit p65 protein expression in group a–e was sorted as $b > d > c > e > a$, which was definite in negative correlation to Sec level (Figure 3b,d). The encouraging results came to a fact that the maintenance of an appropriate concentration of Sec was critical

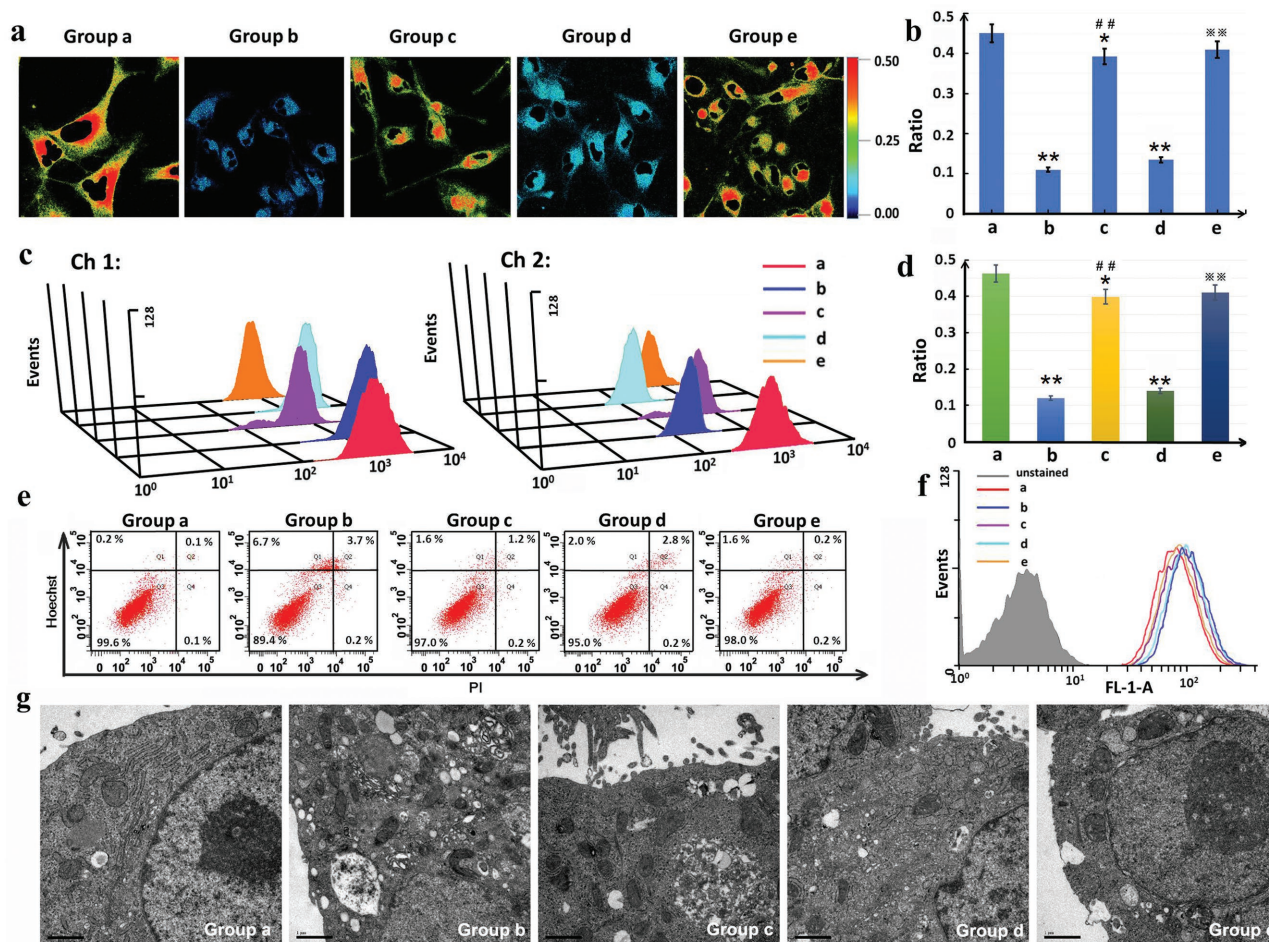


Figure 3. Qualitative analysis of Sec fluctuation in HL-7702 cells by confocal imaging and flow cytometry analysis. a) Pseudocolor ratio images of Sec fluctuation and b) the ratio of mean fluorescence intensities of two different detection channels in HL-7702 cells. All the cells were stained by 10×10^{-6} M Cy-SS for imaging. Pseudocolor ratio images indicated the ratio of channel 2 versus channel 1 at the same time point by confocal laser-scanning microscope with an objective lens ($\times 40$). Fluorescence collection windows for channel 1: 750–800 nm ($\lambda_{\text{ex}} = 730$ nm), channel 2: 690–740 nm ($\lambda_{\text{ex}} = 635$ nm). Scale bar: 10×10^{-6} M. c) Flow cytometry analysis for quantitative application by 10×10^{-6} M Cy-SS and d) the ratio of mean fluorescence intensities of two different detection channels. e) Apoptosis and necrosis analysis of HL-7702 cells by Hoechst 33342/PI staining. Q1): apoptosis, Q2): necrosis, Q3): viable. f) Histograms of NF- κ B immunofluorescence response. g) Transmission electron microscopy observation of the acute and chronic inflammation cells (Scale bar: 1×10^{-6} M). The experiments were repeated three times and the data were shown as mean (\pm S.D.). The differences were performed using a one-way ANOVA. * $p < 0.05$, ** $p < 0.01$ on any other groups versus group a; # $p < 0.05$, ## $p < 0.01$ on group c versus group b; * $p < 0.05$, ** $p < 0.01$ on group e versus group d.

for controlling oxidative stress and inhibiting cellular inflammatory process. The morphological results of mitochondrial swelling caused by apoptosis and necrosis in group b and d were observed by transmission electron microscopy (TEM) (Figure 3g). The results further proved the cell-protection effect of Sec during inflammatory process. Therefore, the ratio fluorescence signals of Sec could be potentially used to accurately diagnose the degrees of inflammation. It also could be utilized as a facilitative tool to assess the therapeutic effects of organoselenium drugs in targeting organs.

2.6. Evaluation of Sec in Mice Model of Acute Hepatitis

As shown in Figure S11 in the Supporting Information, we carried out research on the imaging detection of Sec in peritoneal

cavity of mice BALB/c. The results indicated that our probe could achieve deep tissue imaging in vivo. Next, we strived to investigate the changes of Sec in mice model of acute hepatic inflammation. In order to achieve the targeting detection in liver, we introduced a galactose moiety with liver localization function in our probe Cy-SS for the detection of Sec in liver, because ASGP-R specifically expresses on the plasma membrane of mammalian hepatocytes and selectively recognizes termination of galactose.^[18] The fluorescent images were collected from two fluorescence collection windows, channel 1: $\lambda_{\text{ex}} = 730$ nm with filter 780 nm, and channel 2: $\lambda_{\text{ex}} = 610$ nm with filter 710 nm. As illustrated in Figure 4a, the mice in group a were intravenous injected 50 μ L solution (1:99 DMSO/saline, v/v) as control (DMSO, dimethyl sulfoxide). The mice in group b were given intravenous injection of Cy-SS (10×10^{-6} M, 50 μ L, in 1:99 DMSO/saline, v/v) for 15 min. Probe Cy-SS perfectly

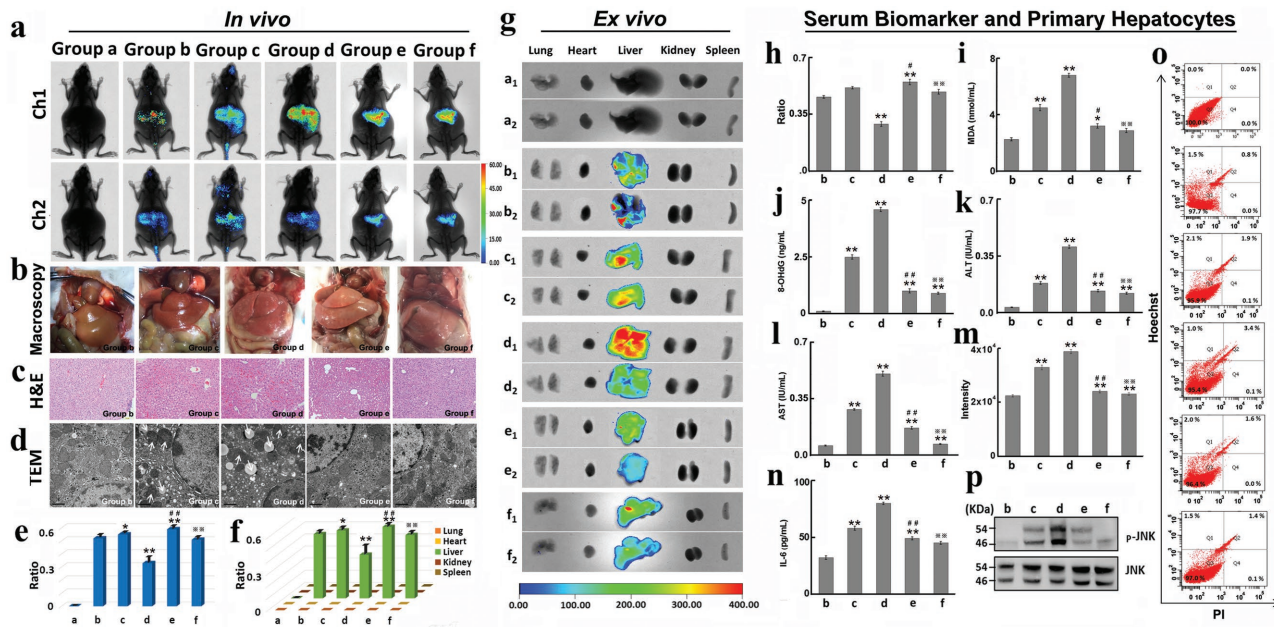


Figure 4. Evaluation of Sec in mice model of acute hepatitis. a) In vivo imaging: Group a: BALB/c mice injected with 50 μL solution (1:99 DMSO/saline, v/v) for 15 min; Group b: BALB/c mice injected with Cy-SS (10×10^{-6} M, 50 μL , in 1:99 DMSO/saline, v/v) for 15 min before imaging; Group c: CCl_4 -induced 6 h acute hepatitis BALB/c mice before the same treat as b; Group d: CCl_4 -induced 24 h acute hepatitis BALB/c mice before the same treat as b; Group e: BALB/c mice were pretreated with 500 $\mu\text{g kg}^{-1}$ selenocystine (i.p.) in PBS daily for eight weeks before the same treat as group c; Group f: BALB/c mice were pretreated with 500 $\mu\text{g kg}^{-1}$ selenocystine (i.p.) in PBS daily for eight weeks before the same treat as group d. b) Ex vivo imaging of Sec in organs sacrificed from group a–f. c) Macropathology images of group b–f. d) Representative slides of H&E-stained liver tissue from group b–f. Scale bar: 100×10^{-6} m. e) TEM observation of group a–d. Scale bar: 1×10^{-6} m. f) Average ratio intensity value of group a–f. g) Ratio analysis of corresponding organs in group a–f. h) Average ratio intensity value of primary hepatocytes obtained from group b–f by Cy-SS. i) Malondialdehyde (MDA) levels in liver serum of group b–f. j) 8-Hydroxy-2'-deoxyguanosine (8-OHdG) levels assessed with an ELISA kit in DNA extracted from liver homogenate in group b–f. k) Alanine aminotransferase (ALT) levels in serum of group b–f. l) Aspartate transaminase (AST) levels in serum of group b–f. m) The mean fluorescence intensity of NF- κB immunofluorescence response in primary hepatocytes by rabbit anti-phospho-NF κB p65(Ser276)/FITC. n) Interleukin-6 (IL-6) levels in serum of group b–f. o) Apoptosis and necrosis analysis of primary hepatocytes of group b–f by Hoechst 33342/PI staining. Q1): apoptosis, Q2): necrosis, Q3): viable. p) JNK activation assessed by separating proteins by SDS–PAGE and immunoblotting with a specific antibody to detect p-JNK (phospho-SAPK/JNK). The experiments were repeated five times and the data were shown as mean (\pm S.D.). The differences were performed using a one-way ANOVA. * $p < 0.05$, ** $p < 0.01$ on any other groups versus group b; # $p < 0.05$, ## $p < 0.01$ on group e versus group c; *** $p < 0.05$, **** $p < 0.01$ on group f versus group d.

targeted in liver indicating its excellent liver targeting capabilities. Ex vivo imaging further affirmed the distinctly selective localization in liver rather than other organs including lung, heart, spleen, and kidney (Figure 4b). The strong fluorescent intensity in channel 2 of group b revealed the high concentration of Sec in normal mice liver (Figure 4a). The average ratio intensity of group b was 0.52 (Figure 4e). The results were consistent with the data of primary hepatocytes in Figure 2b. Acute hepatitis is a kind of serious clinical disease which can cause massive apoptosis and necrosis of liver cells in a short time. This disease can impair liver function severely and lead to liver failure, shock, and ultimate death eventually. Therefore, it is urgent to develop new technology for the accurate and rapid diagnosis of acute hepatitis.

Next, Cy-SS was applied to image Sec in mice model of acute hepatitis. Acute hepatitis was induced by intraperitoneal injection (i.p.) of CCl_4 .^[35] In liver, CCl_4 could be metabolized to trichloromethyl free radical ($\cdot\text{CCl}_3$) in the presence of oxygen. Then $\cdot\text{CCl}_3$ quickly converted into peroxy radical ($\cdot\text{OOCCL}_3$). Its metabolites could covalently bind to macromolecules and initiate lipid peroxidation, which subsequently triggered apoptosis and necrosis of hepatocytes. Mice models of acute hepatitis

in group d were induced by intraperitoneal injection of CCl_4 (0.3 mL kg^{-1} , 50% v/v in liquid paraffin) for 24 h. The macropathology image of group d showed that many gray necrotic dots spread all over liver, which indicated the successful establishment of acute hepatitis (Figure 4c). The results of hematoxylin-eosin staining (H&E) were also used to evaluate acute hepatitis (Figure 4d). And TEM showed the cellular lipid globules and mitochondrial swelling in group b (Figure 4e), which further illustrated the successful establishment of the acute hepatitis model. After intravenously injected Cy-SS (10×10^{-6} M, 50 μL , in 1:99 DMSO/saline, v/v) for 15 min, the mice of group d showed faint fluorescence in channel 2 (Figure 4a). The average value of the ratio image of group d was 0.33, indicating the lower concentration of Sec in acute hepatitis than normal mice in group b (Figure 4f). Since Sec exhibited protective effects in acute hepatitis, we hypothesized that the levels of Sec could not be blindly reduced during the development of the disease. To further check the changes of Sec concentration in the early stage of acute hepatitis, the mice in group c were treated as described in group d, but the test time point was selected at 6 h after injection. As shown in group c, the fluorescence intensity in channel 2 was higher than group d. The average value of

the ratio imaging in group c was 0.55, which was clearly higher level of Sec than those of b and d. This expected result explicitly demonstrated that the self-protect mechanism of liver could upregulate the Sec concentrations during early stage of inflammation process.

Organoselenium drugs which can be metabolized to Sec have been widely used in the treatment of many diseases, owing to its antioxidative ability and anti-inflammatory activity.^[36] Selenocystine is one of such organoselenium compounds, which can diminish the hepatotoxic effects of CCl₄.^[35b] The mice in group f were pretreated with selenocystine (500 μg kg⁻¹ in phosphate-buffered saline (PBS) daily for eight weeks, i.p.). Then these mice were treated as described in group d. The fluorescence intensity in channel 2 of group f was pretty higher than that of group d (Figure 4a), and the average value of the ratio imaging in group f was 0.51 (Figure 4f). The results indicated the higher Sec concentration in group f than that in group d. As shown in macropathology image and H&E, the weakened inflammation of group f was demonstrated (Figure 4c,d), which resulted from the protective effects of selenocystine. The mice of group e were treated as described in group f. The test time was set 6 h. We obtained a higher fluorescence ratio value (0.59) than mice in group f due to the self-protect mechanism of liver. Moreover, the ratio value of group e (0.59) was also higher than that of group c (0.55), which revealed that Sec was an important factor for prevention of acute hepatitis. Ex vivo imaging for liver, lung, heart, spleen, and kidney were displayed in Figure 4b. The macropathology images, H&E, and TEM for mice in group b–f were shown in Figure 4c–e. All the results manifested that our probe Cy-SS could perfectly target in liver. The probe was successfully used to detect the level changes of Sec in normal and acute hepatitis mice. With the support of our probe Cy-SS, we observed the changes of Sec concentration in different inflammation stages of acute hepatitis, which demonstrated that our probe could be employed as a potential diagnostic tool in accurate diagnosis of acute hepatitis.

We next confirmed the correlation between the level of Sec and the development of inflammation in acute hepatitis models. The Sec levels of group b–f were firstly quantified by our probe and then confirmed by LC–MS/MS analysis. The levels of malondialdehyde (MDA) and 8-hydroxy-2'-deoxyguanosine (8-OHdG) were measured to assess the degree of lipid peroxidation damage. Alanine aminotransferase (ALT) and aspartate transaminase (AST) levels were tested to certificate the liver physiological functions. And the stages of acute hepatitis were examined using the levels of NF-κB secretion and interleukin-6 (IL-6). The cellular apoptosis and necrosis were analyzed by Hoechst 33342/propidium iodide (PI) staining via flow cytometry. The activation of primary transcription factor cJun NH₂-terminal kinase (JNK) could induce stress-responsive kinases and lead to inflammation and apoptosis. This factor was investigated by Western blotting.

Primary hepatocytes in group b–f were isolated for flow cytometry analysis to determine the intracellular concentrations of Sec. As shown in Figure 4h, the Sec concentrations in primary hepatocytes of group b–f were consistent with the in vivo imaging results (Figure 4f). The Sec concentrations were sorted in an order: group e > c > b > f > d. The results were also confirmed through LC–MS/MS analysis (Figure S13 and

Table S2, Supporting Information). MDA level was detected by thiobarbituric acid reactive substances assay (Figure 4i). 8-OHdG was assessed with an ELISA kit in DNA extracted from liver homogenate (Figure 4j). The results of MDA and 8-OHdG were all presented in an order of group d > c > e > f > b. This results confirmed that Sec could contribute to protect cells from oxidation damage which caused by acute hepatitis. The ALT and AST levels in serum were also in correlation with the peroxidation damage order (Figure 4k,l). The secretion of NF-κB p65 (Ser276)/FITC. The levels of NF-κB and pro-inflammatory cytokine IL-6 in serum of BALB/c mice provided the same orders (Figure 4m,n) compared with the degree of oxidation damage in Figure 4I,j. All the results indicated that Sec was important for the prevention and treatment effects in acute hepatitis. The development of acute hepatitis induced by CCl₄ was always together with cellular apoptosis and necrosis.^[37] We performed flow cytometry to access apoptosis and necrosis status of the primary hepatocytes. The cells were harvested from the mice in group b–f. All the primary hepatocytes were stained with Hoechst 33342/PI. The order of apoptosis and necrosis percentage was sorted as d > c > e > f > b (Figure 4o). Western blotting illustrated that the factor JNK was activated in group c and d and inactivated in group e and f (Figure 4p). The two results in Figure 4n,o demonstrated that Sec was critical to inhibit the cellular apoptosis and necrosis during acute inflammation process. All the above experiments offered us a fact that Sec played important antioxidant and anti-inflammatory roles during inflammatory process. The accurate diagnosis of inflammation would be benefited from the fluorescence imaging analysis by our probe.

3. Conclusion

In summary, we have developed a ratiometric NIR fluorescent probe (Cy-SS) for qualitative and quantitative detection of Sec in living cells and in vivo. The selenium–sulfur exchange reaction between Cy-SS and Sec can trigger the mechanism of ICT following a color change from green to blue. The probe Cy-SS has been successfully applied to accurately quantitative detection of Sec in living HepG2, HL-7702 cells and primary mouse hepatocytes. And the analysis results are confirmed by flow cytometry and LC–MS/MS. The probe is next used to investigate the fluctuations of Sec in hepatitis cell models. The physiological protective effects of Sec in acute and chronic inflammation cell models are also evaluated by immunofluorescence method. Finally, the probe Cy-SS is employed to target liver and detect Sec concentrations in normal and acute hepatitis BALB/c mice models. Based on our experimental results, we find that Sec is critical to maintain the redox statues of liver and protect liver from inflammatory injury. Since the probe can be used to imaging detection of Sec in the prevention and treatment of inflammation, we hope that this new probe would behave as a precise diagnostic tool in understanding the physiological and pathological roles of Sec in vivo. We believe that such ratiometric NIR fluorescence probes can be applied to qualitatively and quantitatively image the toxic substances and essential cellular components, including small chemical species correlated

with various human diseases in a wide range of chemical, biological, medical, and environmental applications.

Supporting Information

Supporting Information is available from the Wiley Online Library or from the author.

Acknowledgements

The authors thank the National Nature Science Foundation of China (No. 21405172, No. 21575159, and No. 21275158), the program of Youth Innovation Promotion Association, CAS (Grant 2015170), and State Key Laboratory of Environmental Chemistry and Ecotoxicology, Research Center for Eco-Environmental Sciences, CAS (Grant KF2016-22).

Conflict of Interest

The authors declare no conflict of interest.

Keywords

inflammation, near-infrared fluorescent probes, protective effects, selenocysteine

Received: February 11, 2017
Revised: April 16, 2017
Published online: May 24, 2017

- [1] E. E. Battin, J. L. Brumaghim, *Cell Biochem. Biophys.* **2009**, *55*, 1.
- [2] F. Yu, P. Li, G. Li, G. Zhao, T. Chu, K. Han, *J. Am. Chem. Soc.* **2011**, *133*, 11030.
- [3] a) C. Jacob, G. I. Giles, N. M. Giles, H. Sies, *Angew. Chem. Int. Ed.* **2003**, *42*, 4742; b) M. Muttenthaler, P. F. Alewood, *J. Pept. Sci.* **2008**, *14*, 1223; c) T. Nauser, D. Steinmann, W. H. Koppenol, *Amino Acids* **2012**, *42*, 39.
- [4] J. Lu, A. Holmgren, *J. Biol. Chem.* **2009**, *284*, 723.
- [5] M. P. Rayman, *Lancet* **2012**, *379*, 1256.
- [6] a) M. Laclaustra, A. Navas-Acien, S. Stranges, J. M. Ordovas, E. Guallar, *Environ. Health Perspect.* **2009**, *117*, 1409; b) S. Misra, M. Boylan, A. Selvam, J. E. Spallholz, M. Bjornstedt, *Nutrients* **2015**, *7*, 3536.
- [7] A. S. Rahmanto, M. J. Davies, *IUBMB Life* **2012**, *64*, 863.
- [8] Z. Huang, A. H. Rose, P. R. Hoffmann, *Antioxid. Redox Signaling* **2012**, *16*, 705.
- [9] F. Li, P. B. Lutz, Y. Pepelyayeva, E. S. J. Arner, C. A. Bayse, S. Rozovsky, *Proc. Natl. Acad. Sci. USA* **2014**, *111*, 6976.
- [10] a) R. Dhanarajan, P. Abraham, B. Isaac, *Basic Clin. Pharmacol. Toxicol.* **2006**, *99*, 267; b) C. W. Nogueira, J. B. T. Rocha, *Arch. Toxicol.* **2011**, *85*, 1313.
- [11] E. A. Wilhelm, C. R. Jesse, S. S. Roman, C. W. Nogueira, L. Savegnago, *Exp. Mol. Pathol.* **2009**, *87*, 20.
- [12] L. P. Borges, V. C. Borges, A. V. Moro, C. W. Nogueira, J. B. T. Rocha, G. Zeni, *Toxicology* **2005**, *210*, 1.
- [13] N. Uzma, B. S. Kumar, K. I. Priyadarsini, *Biol. Trace Elem. Res.* **2011**, *142*, 723.
- [14] a) M. F. Juette, D. S. Terry, M. R. Wasserman, Z. Zhou, R. B. Altman, Q. Zheng, S. C. Blanchard, *Curr. Opin. Chem. Biol.* **2014**, *20*, 103; b) W. Xu, Z. Zeng, J. H. Jiang, Y. T. Chang, L. Yuan, *Angew. Chem. Int. Ed.* **2016**, *55*, 13658; c) J. Zhou, H. Ma, *Chem. Sci.* **2016**, *7*, 6309; d) W. Sun, S. Guo, C. Hu, J. Fan, X. Peng, *Chem. Rev.* **2016**, *116*, 7768; e) X. Chen, F. Wang, J. Y. Hyun, T. Wei, J. Qiang, X. Ren, I. Shin, J. Yoon, *Chem. Soc. Rev.* **2016**, *45*, 2976; f) M. H. Lee, J. S. Kim, J. L. Sessler, *Chem. Soc. Rev.* **2015**, *44*, 4185; g) Y. Tang, D. Lee, J. Wang, G. Li, J. Yu, W. Lin, J. Yoon, *Chem. Soc. Rev.* **2015**, *44*, 5003.
- [15] X. Chen, Y. Zhou, X. Peng, J. Yoon, *Chem. Soc. Rev.* **2010**, *39*, 2120.
- [16] a) H. Maeda, K. Katayama, H. Matsuno, T. Uno, *Angew. Chem. Int. Ed.* **2006**, *45*, 1810; b) B. Zhang, C. Ge, J. Yao, Y. Liu, H. Xie, J. Fang, *J. Am. Chem. Soc.* **2015**, *137*, 757; c) Q. Sun, S. H. Yang, L. Wu, Q. J. Dong, W. C. Yang, G. F. Yang, *Anal. Chem.* **2016**, *88*, 6084; d) H. Chen, B. Dong, Y. Tang, W. Lin, *Chemistry* **2015**, *21*, 11696.
- [17] a) J. H. Watkinson, *Anal. Chem.* **1966**, *38*, 92; b) F. Kong, B. Hu, Y. Gao, K. Xu, X. Pan, F. Huang, Q. Zheng, H. Chen, B. Tang, *Chem. Commun.* **2015**, *51*, 3102.
- [18] X. Han, F. Yu, X. Song, L. Chen, *Chem. Sci.* **2016**, *7*, 5098.
- [19] F. Yu, P. Li, P. Song, B. Wang, J. Zhao, K. Han, *Chem. Commun.* **2012**, *48*, 4980.
- [20] R. E. Huber, R. S. Criddle, *Arch. Biochem. Biophys.* **1967**, *122*, 164.
- [21] a) D. Steinmann, T. Nauser, W. H. Koppenol, *J. Org. Chem.* **2010**, *75*, 6696; b) T. Nauser, D. Steinmann, W. H. Koppenol, *Amino Acids* **2012**, *42*, 39.
- [22] a) J. H. Lee, C. S. Lim, Y. S. Tian, J. H. Han, B. R. Cho, *J. Am. Chem. Soc.* **2010**, *132*, 1216; b) B. Zhu, X. Zhang, Y. Li, P. Wang, H. Zhang, X. Zhuang, *Chem. Commun.* **2010**, *46*, 5710; c) C. S. Lim, G. Masanta, H. J. Kim, J. H. Han, H. M. Kim, B. R. Cho, *J. Am. Chem. Soc.* **2011**, *133*, 11132; d) J. Fan, Z. Han, Y. Kang, X. Peng, *Sci. Rep.* **2016**, *6*, 19562.
- [23] L. Zhai, J. Liang, X. Guo, Y. Zhao, C. Wu, *Chemistry* **2014**, *20*, 17507.
- [24] a) M. H. Lee, J. H. Han, J. H. Lee, H. G. Choi, C. Kang, J. S. Kim, *J. Am. Chem. Soc.* **2012**, *134*, 17314; b) M. H. Lee, H. M. Jeon, J. H. Han, N. Park, C. Kang, J. L. Sessler, J. S. Kim, *J. Am. Chem. Soc.* **2014**, *136*, 8430; c) L. Zhang, D. Duan, Y. Liu, C. Ge, X. Cui, J. Sun, J. Fang, *J. Am. Chem. Soc.* **2014**, *136*, 226; d) L. Huang, Y. Chen, B. Liang, B. Xing, G. Wen, S. Wang, X. Yue, C. Zhu, J. Du, X. Bu, *Chem. Commun.* **2014**, *50*, 6987.
- [25] F. Yu, P. Li, P. Song, B. Wang, J. Zhao, K. Han, *Chem. Commun.* **2012**, *48*, 2852.
- [26] L. Cesaratto, C. Vascotto, S. Calligaris, G. Tell, *Ann. Hepatol.* **2004**, *3*, 86.
- [27] a) Y. Ogasawara, G. Lacourciere, T. C. Stadtman, *Proc. Natl. Acad. Sci. USA* **2001**, *98*, 9494; b) Y. Kobayashi, Y. Ogra, K. Ishiwata, H. Takayama, N. Aimi, K. T. Suzuki, *Proc. Natl. Acad. Sci. USA* **2002**, *99*, 15932.
- [28] J. R. Encinar, D. Schaumlöffel, Y. Ogra, R. Lobinski, *Anal. Chem.* **2004**, *76*, 6635.
- [29] J. Gaudie, D. N. Sauder, K. P. McAdam, C. A. Dinarello, *Immunology* **1987**, *60*, 203.
- [30] C. A. Feghali, T. M. Wright, *Front. Biosci.* **1997**, *2*, 12.
- [31] J. Gaudie, D. N. Sauder, K. P. McAdam, C. A. Dinarello, *Immunology* **1987**, *60*, 203.
- [32] K. Hesse-Bähr, I. Dreher, J. Köhrle, *Biofactors* **2000**, *11*, 83.
- [33] N. Uzma, B. S. Kumar, K. I. Priyadarsini, *Biol. Trace Elem. Res.* **2011**, *142*, 723.
- [34] L. H. Duntas, *Horm. Metab. Res.* **2009**, *41*, 443.
- [35] a) L. L. de Zwart, R. C. Hermanns, J. H. Meerman, J. N. Commandeur, P. J. Salemink, N. P. Vermeulen, *Toxicol. Appl. Pharmacol.* **1998**, *148*, 71; b) N. Uzma, B. S. Kumar, K. I. Priyadarsini, *Biol. Trace Elem. Res.* **2011**, *142*, 723.
- [36] R. R. Ramoutar, J. L. Brumaghim, *Cell Biochem. Biophys.* **2010**, *58*, 1.
- [37] J. Shi, K. Aisaki, Y. Ikawa, K. Wake, *Am. J. Pathol.* **1998**, *153*, 515.